

## Thermal stability of azurite and malachite in relation to the formation of mediaeval glass and glazes

R. L. Frost<sup>1\*</sup>, Z. Ding, J.T. Kloprogge and W. N. Martens

*Centre for Instrumental and Developmental Chemistry, Queensland University of Technology, 2 George Street, Brisbane, GPO Box 2434, Queensland 4001, Australia.*

Published as:

Frost, R.L., Z. Ding, J.T. Kloprogge, and W.N. Martens, Thermal stability of azurite and malachite in relation to the formation of mediaeval glass and glazes.

*Thermochimica Acta*, 2002. 390(1-2): p. 133-144.

*Copyright 2003 Elsevier*

---

### Abstract

Azurite and malachite have been extensively used as pigments in ancient and medieval manuscripts, glasses and glazes. The thermal stability of naturally occurring azurite and malachite was determined using a combination of controlled rate thermal analysis combined with mass spectrometry and infrared emission spectroscopy. Both azurite and malachite thermally decompose in six overlapping stages but the behaviour is different for the two minerals. These stages occur around 282, 328, 350, 369, 384 and 840°C for azurite and 250, 321, 332, 345, 362 and 842°C for malachite. The first two stages are associated with the loss of water, whereas stages 3 and 4 result from the simultaneous loss of water and carbon dioxide. The sixth stage is associated with reduction of cupric oxide to cuprous oxide and finally to copper. Infrared emission spectroscopy shows that dehydroxylation occurs before the loss of carbonate and that the thermal decomposition is complete by 375°C. The implication of this research is that in the preparation of glass or glazes using these two hydroxy-carbonate minerals of copper the samples will decompose at low temperatures and any colour formation in the glass is not due to azurite or malachite.

*Key words:* azurite, malachite, controlled rate thermal analysis, differential thermogravimetric analysis

---

---

\* Author to whom correspondence should be addressed (r.frost@qut.edu.au)

## 1. Introduction

Azurite  $\{\text{Cu}^{2+}_3(\text{CO}_3)_2(\text{OH})_2\}$  and malachite  $\{\text{Cu}^{2+}_2(\text{CO}_3)(\text{OH})_2\}$  are both monoclinic hydroxy carbonates of copper. The kinetic behavior of the thermal decomposition of synthetic malachite was investigated by means of CRTA under different conditions of reduced pressure, flowing gases and quasi-isobaric atmospheres [1, 2]. The use of thermogravimetry to assess the effect of mechanochemical activation by dry grinding of malachite determined the mass loss of water and carbon dioxide sep. and/or together for  $\text{Cu}_2(\text{OH})_2\text{CO}_3$  samples untreated and ground for different times [3]. Often the thermal analysis is used to determine the effectiveness of catalyst precursors [4]. The thermal decomposition of basic copper carbonate (malachite;  $\text{CuCO}_3\cdot\text{Cu}(\text{OH})_2$ ) in a dynamic atmosphere of air or nitrogen was studied via TG, DTA and DSC at different heating rates showed that in air  $\text{CuCO}_3\cdot\text{Cu}(\text{OH})_2$  released 0.5  $\text{H}_2\text{O}$  at 195°C, transforming into the azurite structure  $2\text{CuCO}_3\cdot\text{Cu}(\text{OH})_2$ . Decomposition then commenced, through two endothermic steps maximized at 325 and 430°C [5, 6]. Thermogravimetry (TG) and evolved gas analysis (EGA) studies of malachite,  $\text{CuCO}_3\cdot\text{Cu}(\text{OH})_2$  and azurite,  $2\text{CuCO}_3\cdot\text{Cu}(\text{OH})_2$ , heated in He carrier gas at  $10^\circ\text{C min}^{-1}$  show that malachite decomposition in a single step at 380°C, in which  $\text{H}_2\text{O}$  and  $\text{CO}_2$  are lost simultaneously. By contrast, the 2 azurites studied both decomposition under these conditions in 2 approx. equal steps, losing one-half of their  $\text{CO}_2$  and  $\text{H}_2\text{O}$  content in each step [7].

Previous studies have determined the thermal decomposition of azurite and malachite under dynamic conditions. Azurite showed in D.T.A. endothermic effects at 420 and at 1100°C, malachite at 390 and at 1190°C, and the pseudomorph of malachite after azurite at 370 and 1085°C. At the 1st endothermic effect, tenorite is formed; at the 2nd endothermic effect, reduction of  $\text{CuO}$  into  $\text{Cu}_2\text{O}$  takes place with constancy of wt. being reached at 660°C. It was found that the volatile ingredients,  $\text{CO}_2$  and  $\text{H}_2\text{O}$ , were released simultaneously [8]. Whereas early studies have shown that the thermal decomposition occurred at temperatures below 200°C [9]. Azurite and malachite were two minerals used as coloring chemicals in ancient manuscripts, glass, tiles and ceramic materials [10-12]. However the thermal analysis of naturally occurring azurite and malachite is very limited, particularly using modern thermo-analytical techniques. This paper reports the thermal, mass spectrometric and infrared emission analyses of the thermal decomposition of azurite and malachite.

## 2. Experimental techniques

### 2.1 Origin of samples

The azurite was obtained from Girilambone copper mine, Girilambone, North of Nyngn, NSW. The malachite was obtained from Burra, South Australia. The samples were analysed for phase purity by X-ray diffraction and for composition by ICP-AES. The samples were found to be phase pure and analysed close to the theoretical composition.

## 2.2 Thermal Analysis

Thermal decomposition of the basic copper carbonate minerals was carried out in a TA high-resolution thermogravimetric analyzer (series Q500) in a flowing nitrogen atmosphere (80 cm<sup>3</sup>/min) at a pre-set, constant decomposition rate of 0.15 mg/min. (Below this threshold value the samples were heated under dynamic conditions at a uniform rate of 2.0 °C/min). The samples were heated in an open platinum crucible at a rate of 2.0 °C/min<sup>-1</sup> up to 300°C. With the quasi-isothermal, quasi-isobaric heating program of the instrument the furnace temperature was regulated precisely to provide a uniform rate of decomposition in the main decomposition stage. The TGA instrument was coupled to a Balzers (Pfeiffer) mass spectrometer for gas analysis. Selected gases only were analyzed.

## 2.3 Infrared emission spectroscopy

FTIR emission spectroscopy was carried out on a Nicolet spectrometer equipped with a TGS detector, which was modified by replacing the IR source with an emission cell. A description of the cell and principles of the emission experiment have been published elsewhere. [13-17] Approximately 0.2 mg of the basic copper carbonate mineral was spread as a thin layer (approximately 0.2 microns) on a 6 mm diameter platinum surface and held in an inert atmosphere within a nitrogen-purged cell during heating.

In the normal course of events, three sets of spectra are obtained: firstly the black body radiation over the temperature range selected at the various temperatures, secondly the platinum plate radiation is obtained at the same temperatures and thirdly the spectra from the platinum plate covered with the sample. Normally only one set of black body and platinum radiation is required. The emittance spectrum (E) at a particular temperature was calculated by subtraction of the single beam spectrum of the platinum backplate from that of the platinum + sample, and the result ratioed to the single beam spectrum of an approximate blackbody (graphite). The following equation was used to calculate the emission spectra.

$$E = -0.5 * \log \frac{Pt - S}{Pt - C}$$

This spectral manipulation is carried out after all the spectral data has been collected. The emission spectra were collected at intervals of 25°C over the range 100 - 750 °C. The time between scans (while the temperature was raised to the next hold point) was approximately 100 seconds. It was considered that this was sufficient time for the heating block and the powdered sample to reach temperature equilibrium. The spectra were acquired by coaddition of 64 scans for the whole temperature range (approximate scanning time 45 seconds), with a nominal resolution of 4 cm<sup>-1</sup>. Good quality spectra can be obtained providing the sample thickness is not too large. If too large a sample is used then the spectra become difficult to interpret because of the presence of combination and overtone bands. Spectral manipulation such as baseline adjustment, smoothing and normalisation was performed using the GRAMS® software package (Galactic Industries Corporation, Salem, NH, USA).

### 3. Results and discussion

Previous studies of the thermal decomposition of malachite are varied and the results depend upon the way the experiments are undertaken. Wide variation in the interpretation of the results for naturally occurring malachite is reported [7-9]. **Figure 1** shows the thermal decomposition of azurite and malachite respectively. The figure also shows the thermal decomposition of copper carbonate for comparison. The results of the stages of the thermal decomposition are shown in **Table 1**. Six stages of decomposition are identified (a) firstly in the 180 to 430°C region and (b) in the ~840°C region. The first five stages for the low temperature decomposition are illustrated in **Figures 2 and 3**. These figures show the peak component analysis of the differential weight loss of azurite and malachite respectively. The theoretical weight loss of azurite based upon the formula  $\{Cu^{2+}_3(CO_3)_2(OH)_2\}$  is 5.2 % for the OH units and 25.5% for the CO<sub>2</sub>, making a total of 30.7%. The theoretical weight loss for malachite based upon the formula  $\{Cu^{2+}_2(CO_3)(OH)_2\}$  is 8.1% for the OH units and 19.9% for the CO<sub>2</sub>, making a total of 28%. The measured weight losses for azurite and malachite are 28.5% and 28.9% respectively. Thus the measured weight loss for malachite is very close to the theoretical value and the weight loss for azurite is less than the predicted value. In the case of malachite the small difference might be accounted for by adsorbed water. An additional weight loss step is observed at 840°C and the weight loss was 8.2 % for malachite and 6.4 % for azurite.

Six weight loss steps are observed for azurite and malachite. The first weight loss step for malachite is 1.7% of the total weight loss and is attributed to the loss of hydroxyl units. **Figures 4 and 5** display the mass spectrometric analyses of the evolved gases for azurite and malachite. Mass spectrometry shows that water is the only evolved gas at this step for malachite and azurite. Some dehydroxylation is occurring at this stage. Comparison of the DTGA of copper carbonate and that of azurite is noteworthy. The first weight loss step for azurite corresponds with that of copper carbonate. No copper carbonate was detected by x-ray diffraction. Step 2 is primarily a dehydroxylation step. One possible type of mechanism is displayed in Table 1. Mass spectrometry of both azurite and malachite shows that water vapour is the evolved gas for this step and that water vapour continues to be evolved in later steps. This means the product of the decomposition must contain both carbonate and hydroxyl units. The product of this step might be  $Cu^{2+}_3(CO_3)_2(OH)$  for azurite and  $Cu^{2+}_2(CO_3)_2(OH)$  for malachite. The total weight loss for steps 1 and 2 for malachite is 6.9% which compared with the theoretical value of 8.1% means that 1.2% of the total OH units is lost in later steps.

The temperature in step 3 is 350°C for azurite and 332°C for malachite. In this step both dehydroxylation and decarboxylation is occurring. Mass spectrometry shows that both carbon dioxide and water vapour are the evolved gases for this step. The weight loss for this step is 10.7% for azurite and 9.4% for malachite. Step 5 is similar to step 4 in that both hydroxyl units and carbon dioxide are lost in the thermal transformation. It is suggested that the product of this reaction is copper oxide. Step 6 is the step where deoxygenation of the copper oxide occurs. Mass spectrometry of the evolved oxygen gas shows that the reaction occurs in two steps as is shown in table 1. The thermal decomposition patterns of azurite and malachite are similar but not the same. However differences in the temperature of the decomposition may be

observed. Mass spectrometry shows that dehydroxylation commences at around 250°C and is completed simultaneously with the loss of carbon dioxide at 450°C.

**Stage 3** is observed at 350°C for azurite and at 332°C for malachite. A weight loss of 37.6% is observed for azurite and 32.5% for malachite. For this decomposition stage, the loss of water and carbon dioxide for azurite is simultaneous and follows the same pattern. This is observed around 348°C in the spectrometric analysis. In contrast, although the DTGA pattern shows a single step at 332°C for malachite, the mass spectrometric analysis shows two closely overlapping steps occurring at **355 and 388°C**. Water and carbon dioxide are lost simultaneously for malachite for this stage. Stage 4 is readily observed as a separate step for both azurite and malachite at 369°C and 345°C. The water and carbon dioxide are lost simultaneously for both azurite and malachite. Although the water and carbon dioxide are being lost together, mass spectrometry shows a loss of both water and carbon dioxide at 432°C and this mass loss is in harmony with stage 5.

A sixth stage in the thermal decomposition of natural azurite and malachite is observed at ~840°C. This weight loss is associated with a loss of oxygen with no other evolved gases being observed. This weight loss is associated with the conversion of copper oxide to cuprous oxide and to copper. Such decompositions have previously been reported at ~660°C [8]. In the dynamic experiment thermal decomposition was reported as single step at 420°C for azurite and at 370°C for malachite[8]. A similar conclusion was reported by others for malachite but azurite was shown to have 2 steps for the thermal decomposition [7]. Mansour proposed a scheme for the thermal decomposition of azurite in which an initial loss of water occurred with a conversion of the azurite to malachite followed by a simultaneous loss of water and carbon dioxide [5]. Such conclusions are in harmony with the results observed in this work. However five steps are observed for the thermal decomposition as opposed to the two steps at 320 and 430°C reported previously [5]. Mansour reported the continuous loss of water and carbon dioxide up to 700°C. In this work, the loss is complete by 430°C for azurite and 400°C for malachite.

### ***Infrared emission spectroscopy of azurite and malachite***

The infrared emission spectra of the hydroxyl-stretching region of azurite and malachite are shown in **Figures 6 and 7**. Three hydroxyl-stretching vibrations in the infrared emission spectra of azurite are identified at 3484, 3426 and 3360  $\text{cm}^{-1}$ . The most intense band is the band at 3426  $\text{cm}^{-1}$ , which corresponds to the Raman band observed at 3420  $\text{cm}^{-1}$ . The intensity of these bands is constant up to 275°C after which the intensity decreases until at 375°C no intensity remains. The hydroxyls are lost in a continuous manner over this temperature range. Four hydroxyl-stretching vibrations are observed in the infrared emission spectra of malachite at 3408, 3358, 3333 and 3134  $\text{cm}^{-1}$ . **Figures 8 and 9** display the carbonate vibrations for azurite and malachite. The intensity of the carbonate remains constant up to 300°C, and then decomposition occurs. A new infrared band is observed at 600  $\text{cm}^{-1}$ . The appearance of this band shows the temperature for the onset of thermal decomposition. **Figure 10** shows the loss of intensity of selected hydroxyl and carbonate bands for azurite and malachite. The figures clearly demonstrate that differences exist between the dehydroxylation and loss of carbon dioxide of the two minerals. The intensity of the hydroxyl bands at 3370, 3427 and 3482  $\text{cm}^{-1}$  for azurite decreases continuously from

225°C. The intensity of the carbonate bands at 1509, 1463 and 1415  $\text{cm}^{-1}$  starts to decrease at a slightly higher temperature. This observation is in harmony with the results of the mass spectrometric analysis where dehydroxylation commences before the loss of carbon dioxide. For malachite the intensity of the IES bands at 3134, 3333, 3358 and 3408  $\text{cm}^{-1}$  decreases over the temperature range 150°C to 375°C at which point no intensity remains in the bands. The intensity of the 1505  $\text{cm}^{-1}$  band shows a significant decrease in intensity at 275°C whereas the 1392  $\text{cm}^{-1}$  band decreases constantly with temperature increase. The significant change in intensity at 275°C of the 1505  $\text{cm}^{-1}$  band shows a phase change in the mineral is occurring at this temperature. This change is associated with the dehydroxylation. The intensity of the 1505  $\text{cm}^{-1}$  band is replaced with an increase in intensity of a band at 1425  $\text{cm}^{-1}$ . The infrared emission spectroscopy also shows that the loss of hydroxyls and the carbon dioxide occurs simultaneously.

#### 4. Conclusions

A number of conclusions are drawn:

- (a) The thermal decomposition of azurite and malachite are similar but not the same.
- (b) This decomposition is complex with five overlapping thermal decomposition steps identified and a sixth at elevated temperatures.
- (c) Stages 1 and 2 result from the loss of water.
- (d) Stages 3 and 4 result from the simultaneous loss of water and carbon dioxide.
- (e) The stages identified in the mass spectrometric analyses are in harmony with the steps identified in the differential thermogravimetric patterns.
- (f) Infrared emission spectroscopy showed that the hydroxyls were lost before the evolution of carbon dioxide.
- (g) Above 325°C, both the hydroxyls and carbon dioxide are lost concurrently
- (h) IES shows that the dehydroxylation is complete by 375°C.

Implications for the use of malachite and azurite from archaeological and mediaeval glasses and glazes rest with the decomposition of these two colouring agents at low temperatures. In any glass or glaze formation these minerals will have decomposed. An alternative methodology depends upon the coating of a surface with azurite or malachite and then placing the clear glass or glaze over this coating.

#### Acknowledgments

The Centre for Instrumental and Developmental Chemistry, of the Queensland University of Technology is gratefully acknowledged for financial, and infra-structural support for this project. The Australian Research Council (ARC) is thanked for the funding of the Integrated Thermal Analysis Facility.

#### REFERENCES

1. N. Koga, J. M. Criado and H. Tanaka, *Thermochim. Acta* 340-341 (1999) 387.
2. N. Koga, J. M. Criado and H. Tanaka, *J. Therm. Anal. Calorim.* 60 (2000) 943.
3. K. Wieczorek-Ciurowa, J. G. Shirokov and M. Parylo, *J. Therm. Anal. Calorim.* 60 (2000) 59.

4. R. H. Hoepfener, E. B. M. Doesburg and J. J. F. Scholten, *Appl. Catal.* 25 (1986) 109.
5. S. A. A. Mansour, *J. Therm. Anal.* 42 (1994) 1251.
6. H. Tanaka and M. Yamane, *J. Therm. Anal.* 38 (1992) 627.
7. I. W. M. Brown, K. J. D. Mackenzie and G. J. Gainsford, *Thermochim. Acta* 75 (1984) 23.
8. W. Kleber, *Krist. Tech.* 2 (1967) 5.
9. D. R. Simpson, R. Fisher and K. Libsch, *Am. Mineralogist* 49 (1964) 1111.
10. R. J. H. Clark, *J. Mol. Struct.* 480-481 (1999) 15.
11. H. G. M. Edwards, D. W. Farwell, F. R. Perez and S. J. Villar, *Appl. Spectrosc.* 53 (1999) 1436.
12. H. G. M. Edwards, D. W. Farwell, F. R. Perez and J. M. Garcia, *Analyst* 126 (2001) 383.
13. R. L. Frost and A. M. Vassallo, *Clays Clay Miner.* 44 (1996) 635.
14. R. L. Frost, J. T. Kloprogge, S. C. Russell and J. Sztetu, *Appl. Spectrosc.* 53 (1999) 829.
15. J. T. Kloprogge and R. L. Frost, *Appl. Clay Sci.* 15 (1999) 431.
16. J. T. Kloprogge, R. L. Frost and J. Kristof, *Can. J. Anal. Sci. Spectrosc.* 44 (1999) 33.
17. J. T. Kloprogge and R. L. Frost, *Neues Jahrb. Mineral., Monatsh.* (2000) 145.

**Table 1**

	<b>azurite</b>	<b>azurite</b>	<b>malachite</b>	<b>malachite</b>		
Weight Loss	Temperature °C %/area	Theoretical weight loss	Temperature °C %/area	Theoretical weight loss	<b>Proposed Thermal reaction of azurite</b> {Cu <sup>2+</sup> <sub>3</sub> (CO <sub>3</sub> ) <sub>2</sub> (OH) <sub>2</sub> }	<b>Proposed Thermal reaction of malachite</b> {Cu <sup>2+</sup> <sub>2</sub> (CO <sub>3</sub> )(OH) <sub>2</sub> }
Step 1	282 3.1	5.2%	250 1.7	8.1%	Loss of CO <sub>2</sub> Probably from some free CuCO <sub>3</sub> present	Loss of OH units as water
Step 2	328 2.5 Total dehydroxylation = 5.6%		321 5.2		Loss of OH units- dehydroxylation Cu <sup>2+</sup> <sub>3</sub> (CO <sub>3</sub> ) <sub>2</sub> (OH) <sub>2</sub> → 2Cu <sup>2+</sup> <sub>3</sub> (CO <sub>3</sub> ) <sub>2</sub> (OH) + H <sub>2</sub> O	Loss of OH units- dehydroxylation {Cu <sup>2+</sup> <sub>2</sub> (CO <sub>3</sub> )(OH) <sub>2</sub> } → 2Cu <sup>2+</sup> <sub>2</sub> (CO <sub>3</sub> ) <sub>2</sub> (OH) + H <sub>2</sub> O
Step 3	350 10.7	25.5%	332 9.4	19.9%	Possible Cu <sup>2+</sup> <sub>3</sub> (CO <sub>3</sub> ) <sub>2</sub> (OH) → CuCO <sub>3</sub> CuO + CO <sub>2</sub> + H <sub>2</sub> O	Cu <sup>2+</sup> <sub>2</sub> (CO <sub>3</sub> ) <sub>2</sub> (OH) → CuCO <sub>3</sub> + CuO + CO <sub>2</sub> + H <sub>2</sub> O
Step 4	369 5.9		345 5.9		Loss of water and carbon dioxide Cu <sup>2+</sup> <sub>3</sub> (CO <sub>3</sub> ) <sub>2</sub> (OH) → CuCO <sub>3</sub> + CO <sub>2</sub> + H <sub>2</sub> O	Loss of water and carbon dioxide Cu <sup>2+</sup> <sub>2</sub> (CO <sub>3</sub> ) <sub>2</sub> (OH) → CuCO <sub>3</sub> + CO <sub>2</sub> + H <sub>2</sub> O
Step 5	384 6.3 Total decarboxylation=22.9		362 6.7 Total decarboxylation = 21.95		Loss of carbon dioxide only CuCO <sub>3</sub> → CuO + CO <sub>2</sub>	Loss of carbon dioxide only CuCO <sub>3</sub> → CuO + CO <sub>2</sub>
Step 6	840°C 8.2		842°C 6.4		Loss of oxygen CuO → Cu <sub>2</sub> O + O <sub>2</sub> Cu <sub>2</sub> O → Cu + O <sub>2</sub>	Loss of oxygen CuO → Cu <sub>2</sub> O + O <sub>2</sub> Cu <sub>2</sub> O → Cu + O <sub>2</sub>





## LIST OF FIGURES

- Figure 1. Thermogravimetric and differential thermogravimetric analyse of azurite, malachite and copper carbonate
- Figure 2. Component analysis of the differential thermogravimetric analysis of azurite
- Figure 3. Component analysis of the differential thermogravimetric analysis of malachite.
- Figure 4. Mass spectrum of water, carbon dioxide and oxygen and the differential thermogravimetric pattern of malachite.
- Figure 5. Mass spectrum of water, carbon dioxide and oxygen and the differential thermogravimetric pattern of azurite.
- Figure 6. Infrared emission spectra of the hydroxyl stretching vibrations of azurite.
- Figure 7. Infrared emission spectra of the hydroxyl stretching vibrations of malachite.
- Figure 8. Infrared emission spectra of the 550 to 1800  $\text{cm}^{-1}$  region of azurite.
- Figure 9. Infrared emission spectra of the 550 to 1800  $\text{cm}^{-1}$  region of malachite.
- Figure 10. Variation of band intensity as a function of temperature.

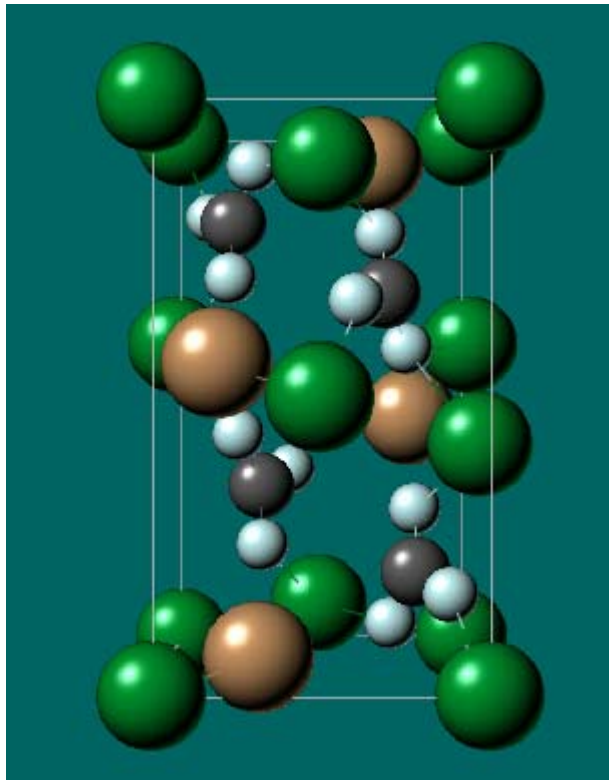


Figure 1